sustainability

MDPI

Article

Mathematical Modeling of the Dynamic Temperature Profile in Geothermal-Energy-Heated Natural Gas Hydrate Reservoirs

Boyun Guo * and He Zhang

Department of Petroleum Engineering, University of Louisiana at Lafayette, Lafayette, LA 70504, USA; he.zhang1@louisiana.edu
* Correspondence: boyun.guo@louisiana.edu

Abstract: An analytical model was developed in this study for predicting the dynamic temperature profile in natural gas hydrate (NGH) reservoirs that receive heat energy from a geothermal layer for accelerating gas production. The analytical model was validated by a comparison of its result to the result given by a numerical model. The expression of the analytical model shows that, for a given system, the heat transfer is proportional to the mass flow rate and the temperature drop along the heat dissipator wellbore. Applying the analytical model to the NGH reservoir in the Shenhu area, Northern South China Sea, allowed for predicting the dynamic temperature profile in the NGH reservoir. The model result reveals that the NGH reservoir temperature should increase quickly at any heat-affected point, but it should propagate slowly in the radial direction. It should take more than two years to dissociate NGH within 20 m of the heat dissipator wellbore due to only thermal stimulation. Therefore, the geo-thermal stimulation method should be used as a technique for accelerating gas production with a depressurization scheme. The formation of gas phase due to the NGH dissociation should reduce the thermal conductivity of the NGH reservoir, while the water phase that dropped out from the dissociation should increase the thermal conductivity. The resultant effect should be investigated in the future in laboratories and/or numerical simulation of the dynamic water-gas two-phase flow coupled with a heat–transfer mechanism.

Keywords: subsea; gas hydrate; production; geothermal method; mathematical modeling

check for updates

Citation: Guo, B.; Zhang, H. Mathematical Modeling of the Dynamic Temperature Profile in Geothermal-Energy-Heated Natural Gas Hydrate Reservoirs. *Sustainability* **2022**, *14*, 2767. https://doi.org/10.3390/su14052767

Academic Editors: Arturo Farfán Martín, Cristina Sáez Blázquez and Ignacio Martín Nieto

Received: 10 February 2022
Accepted: 24 February 2022
Published: 26 February 2022

1. Introduction

Natural gas hydrates (NGH) trap a tremendous amount of natural gas in on shore and offshore reservoirs worldwide. The global stocks of a gas hydrates range account for at least 10 times the supply of conventional natural gas deposits, with between 100,000 and 300,000,000 trillion cubic feet of gas yet to be discovered, and twice as much carbon as Earth's other fossil fuels combined [1]. If these sources of natural gas could be efficiently developed, NGH could potentially displace coal and oil as the top sources of the world's energy [2].

Compared to traditional liquid fossil fuels, the natural gas stored in the NGH is favored even more with its ecologically friendly nature owing to its low-carbon content. The global initiative to restore a low-carbon planet has made NGH more attractive than other energy sources. The tremendous amount of reverse NGH and its cleanness have accounted for its increasing attractiveness to be a promising energy source for the next generations of humankind [3].

Research on NGH has gone a transition from scientific studies [4] through investigations of petrophysical properties and geological characterization of reservoirs [5] to field pilot studies [6]. Field pilots test gas well productivity in NGH reservoirs [7,8]. While these studies continue to deepen people's understanding of properties of NGH reservoirs and challenges in field operations during natural gas extraction from the NGH sediments, efforts are shifting from being stagnant with the documented huge reserve amount [9] to more relevant technical and economic studies on NGH pay zone potentials, gas well productivity, and gas well construction techniques [10–13].

Recently, Japan, China, and India have carried out well testing and gas production from NGH [7,14]. The currently tested methods for exploration and production of natural gas from oceanic NGH include (1) depressurization, (2) thermal stimulation, (3) thermodynamic inhibitor injection, and (4) combination of some of these methods.

The depressurization method decreases the pressure in NGH deposits below the hydrate dissociation pressure [15,16]. The thermal stimulation method uses surface-provided hot water/brine/steam to heat the NGH deposit above hydrate dissociation temperature [17–19]. The thermodynamic inhibitor injection method involves the injection of chemicals, such as salts and alcohols, to change the hydrate pressure–temperature equilibrium conditions [20,21]. The one example of trials using the combined method was reported by Moridis and Reagan [22,23].

The depressurization-based methods are commonly used due to their simplicity, technical effectiveness, and lower cost. However, due to the strong endothermic effect of the dissociation and the Joule–Thompson cooling effect due to the rapidity depressurization, the NGH zone can experience steep local temperature drop and zone-wide temperature decline as the NGH dissociation takes place [3,24]. The work of Kurihara [5] shows that a steep local temperature drop can cause formation of secondary hydrate and ice near the producing wellbore. This would undermine well productivity due to flow restriction/choking the well. The zone-wide temperature decline due to gas expansion can reduce long-term productivity of the well as the in situ temperature deviates from the three-phase equilibrium. Based on computer simulation, Hong and Pooladi-Darvish [25] also reported that the NGH zone can experience a significant decline in temperature because of reservoir cooling due to the endothermic dissociation. Results of their study suggest that heat transfer is the dominant mechanism controlling the NGH dissociation process. This phenomenon was investigated by Moridis and Reagan [22] and verified in field testing by Qin et al. [26]. Therefore, the depressurization-based method requires a slow and graduate change of pressure and temperature to maintain long-term production. Without external heat supply to the NGH zone, it is difficult for the depressurization method to be efficient. Moridis et al. [27] experimented with gas production from 55-ft thick NGH zone by circulating warm water and obtained an increased gas production peaked at 53 Mscfd. The results confirmed that the replenishment of heat into active producing NGH reservoirs can facilitate a longer production life span for the NGH zone.

The currently tested thermal stimulation methods involve heat energy provided by warm water or electricity from the surface. The hydrate dissociation that solely relies on conventional thermal stimulation has been proven not adequate to be sustainable because it is slow, inefficient, and excessively energy demanding. Introducing warm water into the NGH zone could also have adverse effects on the relative permeability to the gas phase. Electrical heating of the NGH zone is even a slower and less efficient process than the water-heating. The use of inhibitors for producing gas from NGH is limited owing to their high cost, short-term effectiveness, and risks of formation damage [20,21].

In summary, none of these methods have been demonstrated to be economical due to low productivity of wells. Other factors affecting the NGH reservoir development include wellbore collapse and excessive sand production. These two issues arose because of reducing wellbore pressure in depressurization and thermal stimulation for improving well productivity. Although some novel ideas have been proposed to solve these problems, including the use of radial lateral wells [28], frac-packed wells [13] and horizontal snake wells [10,12], they have not been tested in the field.

Apparently, the thermal stimulation is the most promising method if the problems of excessive energy-demand and adverse effect of water on the gas relative permeability are solved. Fu et al. [29] proposed a new idea for thermal stimulation using geothermal energy. It involves using y-shaped well couples to transfer the heat in a geothermal reservoir at a deeper depth to the NGH zone through a non-water contacting horizontal lateral hole.

Results of their mathematical modeling show that the temperature in the heating lateral hole can be significantly higher than the dissociation temperature of NGH. However, there is a gap between their mathematical model and well production forecast because the heat transfer efficiency to the NGH zone is not known. This study fills the gap by developing an analytical model for heat transfer into the NGH zone. The analytical model was verified by a numerical model for its correctness.

2. System Description

Figure 1 shows a schematic diagram of a y-shaped well couple proposed by Fu et al. [29] for producing natural gas from a subsea NGH reservoir. Seawater is injected by pump *1* through flexible hose *2* into the water injection well *3* along the inner casing *4* reaching the geothermal zone *8*. The water is heated up to a temperature of the geothermal zone, which is dependent on the depth of geothermal zone. The hot seawater in the heat absorber wellbore *9* travels through the annulus area and arrives at the heat dissipator wellbore *10* located in the gas hydrate zone *12*. The heat of water in the wellbore transfers into the gas hydrate zone. When the temperature in the gas hydrate zone rises to a hydrate dissociation temperature, the dissociated natural gas and liquid flow into the horizontal production wellbore *11*. The natural gas and liquid steam are produced through gas production well *14*. The produced gas and water are collected and released through flexible hose *15* to separator *16*. The liquid stream, which is mainly water, is disposed to the sea. The produced natural gas is compressed by a gas compressor *17* and stored in gas tank *18*, which is later transported to pipeline network *19* or shipped for sale directly. After the heat in the warm water is dissipated into the hydrate formation, the seawater becomes less warm and flows into the annulus of the production well *14*, and is then circulated by pump *1*. Now, the injection seawater has completed a utilization cycle. The connections between the ship and the wellheads are flexible to account for the movement of the ship.

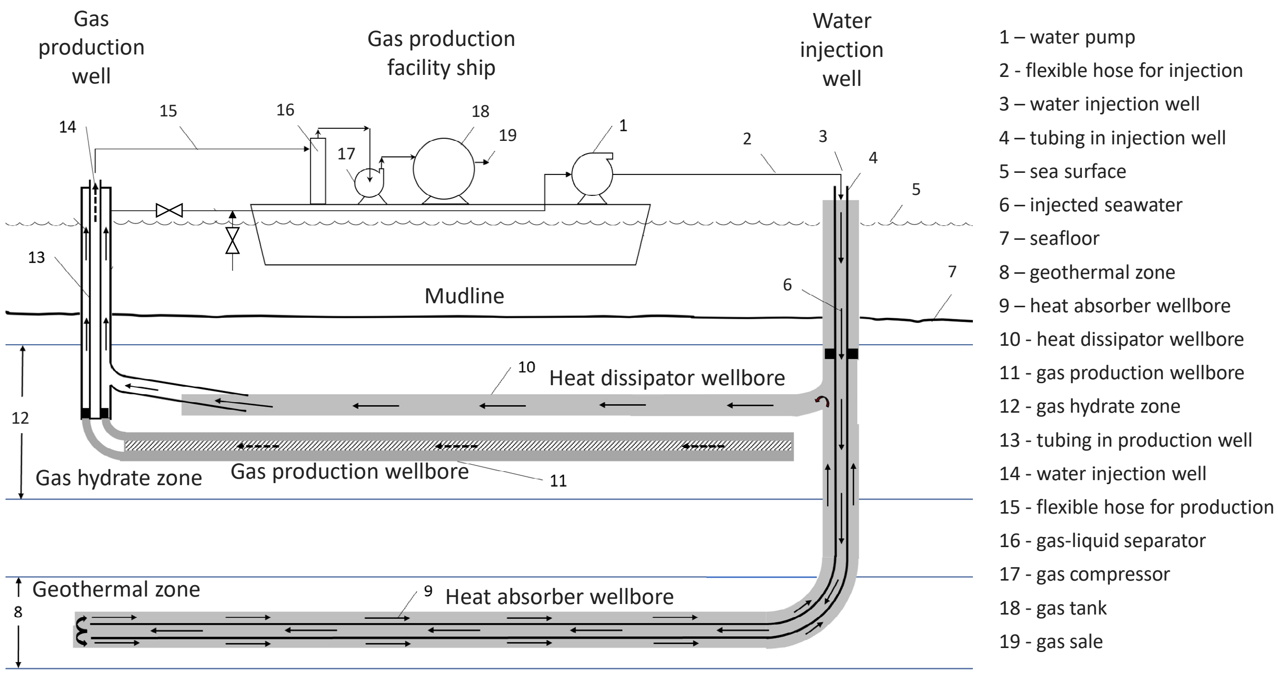

Figure 1. Schematic diagram of a y-shaped well couple for transferring heat from a geothermal zone to a gas hydrate reservoir.

3. Mathematical Models

The system depicted in Figure 1 presents a technique of utilizing geothermal energy through a y-shaped wellbore couple to facilitate the production of natural gas from the NGH reservoir, which eliminates the need to burn fossil fuels or use electricity to heat the injection fluid. This process not only saves energy but also reduces carbon footprint. The gas well productivity depends on the heat transfer efficiency from the heat dissipator wellbore deep into the NGH reservoir where the horizontal production wellbore is placed. An analytical model was developed in the study to quantitively predict the temperature rise in the NGH reservoir. The analytical model verified by a numerical model for its correctness.

Analytical Model. Consider the horizontal heat dissipator wellbore *10* shown in Figure 1. The following assumptions are made for modeling the heat transfer process:

The reservoir is homogeneous and isotropic with constant density, thermal conductivity, and specific heat.

The reservoir is considered infinitely large as compared to the wellbore size.

The governing equation of temperature is the commonly known diffusivity equation expressed as

$$\frac{1}{r}\frac{\partial}{\partial r}\left(r\frac{\partial T}{\partial r}\right) = \frac{1}{\beta}\frac{\partial T}{\partial t} \tag{1}$$

where T is temperature in °C, r is distance from the wellbore center line in meter, t is time in second, and b is thermal diffusivity constant defined by

$$\beta = \frac{K}{\rho_s C_{ps}} \tag{2}$$

where K is rock thermal conductivity in W/m-°C, r_s is rock density in kg/m^3, and C_{ps} is rock heat capacity at constant pressure (specific heat) in J/kg-°C.

The initial condition is expressed as

$$T = T_i \quad \text{at } \ t = 0 \ \text{ for all } \ r \tag{3}$$

where T_i is initial reservoir temperature. The boundary condition at the wellbore is expressed as

$$q_{r_w} = -K\left[\frac{dT}{dr}\right]_{r=r_w} \quad \text{for all } \ t. \tag{4}$$

where q_{rw} is rate of flow of heat per unit time per unit area of wellbore in J/s-m^2. For a circular wellbore with radius r_w and length L, the following relation holds true:

$$q_{r_w} = \frac{Q_{r_w}}{2\pi r_w L} \tag{5}$$

where Q_{rw} is rate of flow of heat per unit time in J/s. Substituting Equation (5) into Equation (4) and rearranging the latter gives

$$\frac{Q_{r_w}}{2\pi LK} = -r_w\left[\frac{dT}{dr}\right]_{r=r_w} \quad \text{for all } \ t. \tag{6}$$

The solution of Equation (1) takes the following form (see Appendix A for derivation):

$$T = T_i + \frac{Q_{r_w}}{4\pi LK}E_i(s) \tag{7}$$

where $Ei(s)$ is exponential integral and

$$s = \frac{r^2}{4\beta t} \tag{8}$$

The heat flow rate from wellbore to reservoir can be calculated by

$$Q_{rw} = C_{pl}\dot{m}_p(T_{in} - T_{out}) \tag{9}$$

where C_{pl} is the heat capacity of the fluid inside the wellbore in J/(kg·°C), $\dot{m}_p$ is the mass flow rate inside the wellbore in kg/s, and T_{in} and T_{out} are fluid temperatures in °C at the inlet and outlet of the wellbore, respectively.

Numerical Model. A two-dimensional numerical model was built in the finite element software COMSOL Multiphysics. Considering the symmetry of the system, the numerical model was set up with the cylindrical coordinates (r-z coordinates) with the horizontal wellbore set in z-direction and heat transfer in the radial r-direction. The governing equation for heat transfer is as follows:

$$\rho C_{ps}\frac{\partial T}{\partial t} + \rho C_{ps}\mathbf{u}\cdot\nabla T + \nabla\cdot\mathbf{q} = Q \tag{10}$$

where r is solid density in kg/m^3, C_{ps} is the heat capacity of the solid in J/(kg·°C), T is temperature in °C, t is time in seconds, $\mathbf{u}$ is velocity field in m/s, $\mathbf{q} = -K\nabla T$, and Q is the heat source in W/m^3.

Figure 2 shows a radial cross-section of a two-dimensional discrete grid system built in the numerical model. The formation rock was assumed to be homogeneous and isotropic. The dimensions of the domain are 10 m of height in the z-direction, 400 m of outer boundary in the r-direction, and 0.3 m of inner boundary in the r-direction (r_w). The initial condition is given by Equation (3) and the inner boundary condition is described by Equation (4). The mesh type of the domain is linear triangular with a minimum element size of 0.02 m and a maximum size of 10 m. The time step size is not defined by the user of COMSOL.

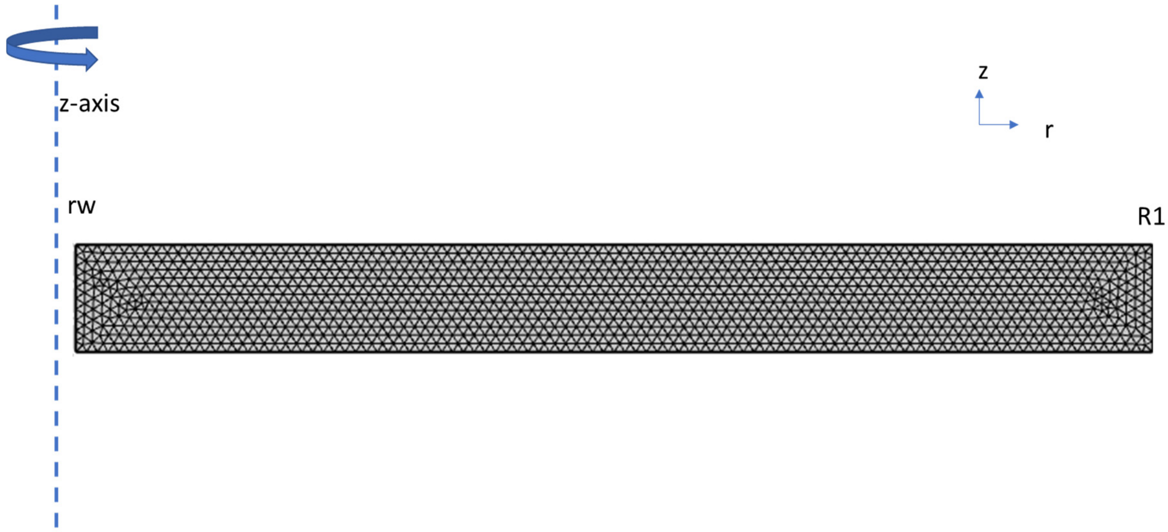

Figure 2. A two-dimensional discrete grid system built in the numerical model.

Model Validation. The analytical model was validated by a comparison of its result and the result given by the numerical model for an arbitrary data set shown in Table 1. A comparison of temperature profiles given by the analytical and numerical models are presented in Figure 3. This comparison indicates that the results given by the two models are identical, which implies the correctness of the analytical model. Figure 4 presents the temperature raise at different radial distances given by the numerical model. It indicates that the rate of temperature increase slows down with time.

Table 1. An input data set for model comparison.

Model Parameter	Value	Unit
Solid density (r_s)	2600	kg/m^3
Solid thermal conductivity (K)	1	W/m-°C
Solid heat capacity (C_{ps})	1	J/kg-°C
Solid initial temperature (T_i)	20	°C
Liquid density (r_L)	1000	kg/m^3
Liquid heat capacity (C_{pl})	1	J/kg-°C
Borehole length (L)	10	m
Borehole radius (r_w)	0.3	m
Liquid flow rate (Q_f)	0.01	m^3/s
Borehole inlet temperature (T_{in})	100	°C
Borehole outlet temperature (T_{out})	30	°C

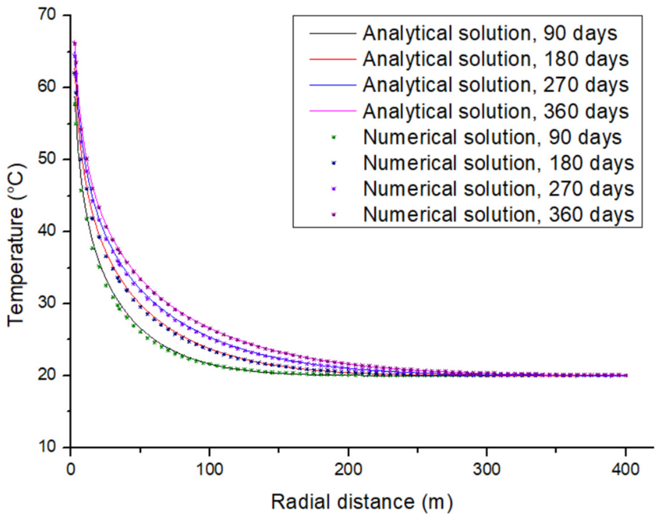

Figure 3. Comparison of results given by the analytical and numerical models.

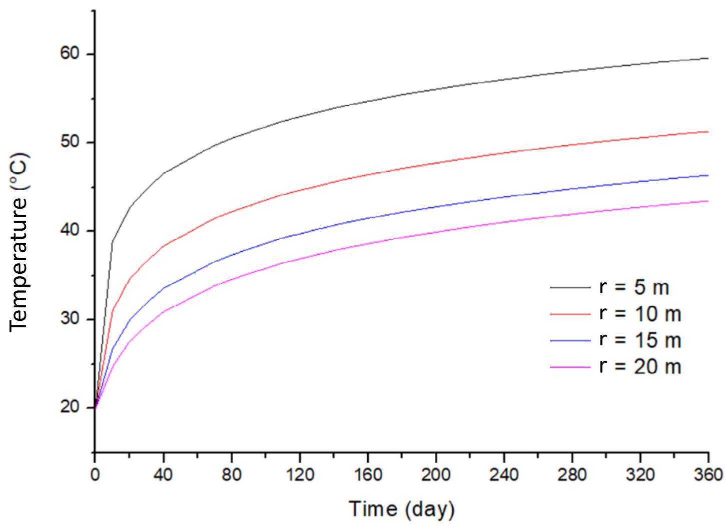

Figure 4. Temperature increase at different radial distances from wellbore.

4. Applications

The mathematical models were employed to predict the temperature increase of an NGH reservoir in the South China Sea in a scenario of using geothermal energy for producing natural gas. The example NGH reservoir is in the Shenhu area, Northern South China Sea. The pay zone is about 1180 m below sea level and 155 m to 177 m under the mud line [30]. The average reservoir pressure and temperature are estimated to be approximately 14 MPa and 6°, respectively. The NGH reservoir is composed of clayey silt in three intervals [31]. The NGH layer in interval "a" has a mean effective porosity 0.35, mean hydrate saturation about 34%, and mean permeability 2.9 md. The layer in interval "b" has a mean effective porosity 0.33, mean hydrate saturation 31%, and mean permeability 1.5 md. The layer in interval "c" has a mean effective porosity 0.32, mean gas saturation 7.8%, and mean permeability 7.4 md.

Assuming that the major component of the natural gas in the Shenhu area is methane, the dissociation temperature of the NGH at 14 MPa is about 15° [32]. Fu et al.'s [29] study shows that, if the heat energy in a geothermal zone (60°) at a vertical depth of 2500 m is brought to the NGH layer with a water circulation rate of 10 kg/s, the temperature of water at the inlet and outlet of a 2000 m long heat dissipator wellbore is predicted to be 47.5° and 36.5°, respectively. To predict the temperature change in the NGH layer with the analytical model, Table 2 was prepared for input data.

Table 2. Input data to the analytical model for the Shenhu NGH reservoir.

Wellbore Length (L)	**2000**	**m**
Thermal conductivity of rock (K)	3.06	W/m-°C
Density of rock (r_s)	2600	kg/m^3
Heat capacity of hydrate zone (c_{ps})	878	J/kg-°C
Initial rock temperature (T_i)	6	°C
Thermal fluid density (r_L)	1030	kg/m^3
Thermal fluid flow rate (Q_f)	0.1	m^3/s
Heat capacity of thermal fluid (C_{pl})	4184	J/kg-°C
Fluid temperature at inlet of wellbore (T_{in})	47.5	°C
Fluid temperature at outlet of wellbore (T_{out})	36.5	°C

Figure 5 presents model-calculated temperature profiles at 10 days, 20 days, and 30 days of water circulation. It indicates that the temperature should increase quickly in the vicinity of wellbore in the first month of water circulation. This is expected for the radial heat flow system.

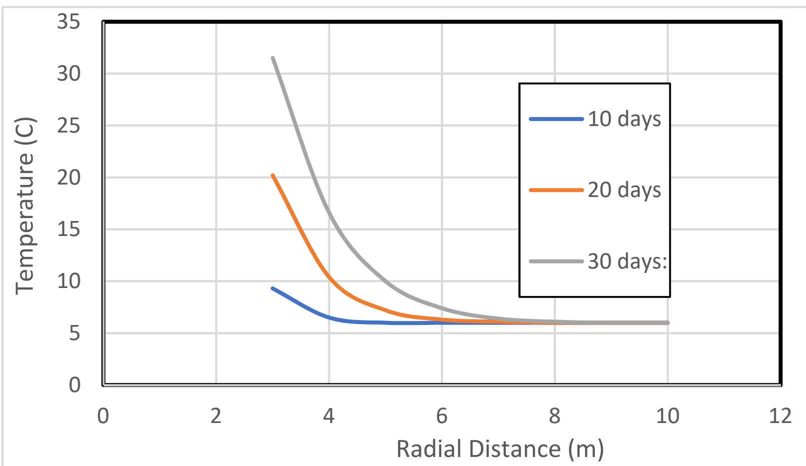

Figure 5. Temperature profiles at a fixed time of water circulation.

Figure 6 shows model-calculated temperature changes with time of water circulation at fixed radial distances. It implies that the temperature at a given radial distance should increase linearly with time after a while of water circulation. This is an indication of an efficient heat transfer process.

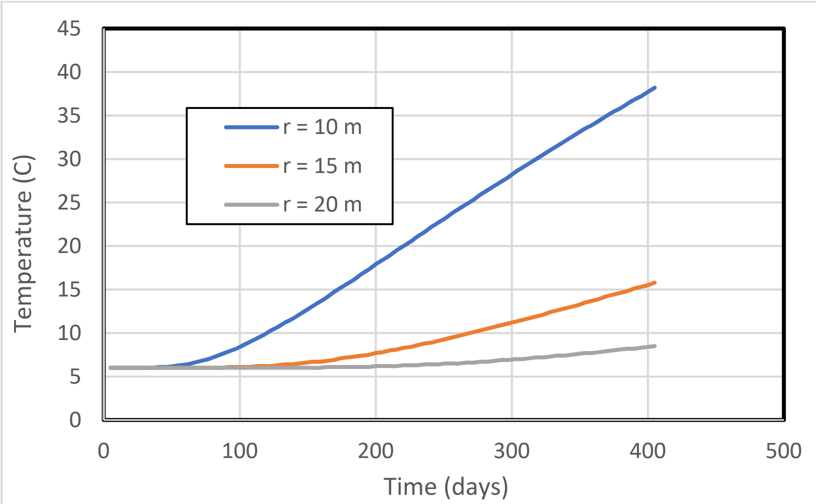

Figure 6. Temperature change with time of water circulation at fixed radial distances.

Figure 7 illustrates the model-calculated propagation of a temperature front of 15 °C (NGH dissociation temperature at the initial reservoir pressure) as a function of time of water circulation. It indicates a nonlinear trend with a declining rate of propagation as the slope of curve drops with time. This again is expected for the radial system of heat flow.

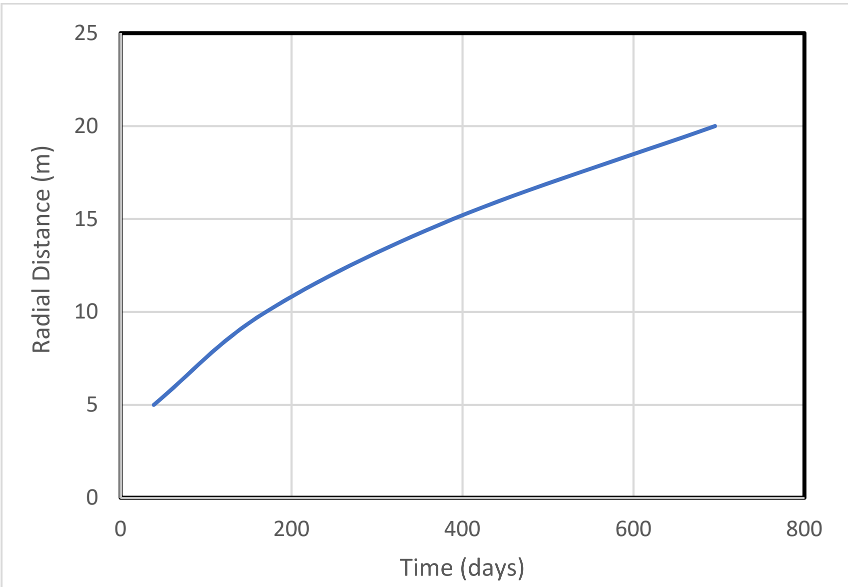

Figure 7. Temperature front of 15 °C as a function of time of water circulation.

5. Discussion

The data presented in Figures 5–7 reveal that the temperature would increase quickly at any heat-affected point, but it would propagate slowly in the radial direction. It would take more than two years to dissociate NGH within 20 m of the heat dissipator wellbore due to only thermal stimulation. This is consistent with the observations by other researchers [20,21] showing that the hydrate dissociation solely relying on thermal stimulation is not adequate to be sustainable because it involves a slow and inefficient heat transfer process in the reservoir rock. Therefore, the geo-thermal stimulation method should be used as a technique for accelerating gas production with a depressurization scheme.

Because real gas law demands that the increase in temperature will increase the pressure of free gas behind the 15 °C front, there is a tendency of reformation of NGH if the pressure fluctuates [32]. This suggests that the natural gas released from the NGH should be produced in time through the gas production wellbore to reduce pressure.

Results presented in this work are from using the data in Table 2. Equations (7) and (9) show that, for a given system, the heat transfer is proportional to the mass flow rate $\dot{m}_p$ and the temperature difference ($T_{in} - T_{out}$). However, this temperature difference is affected by the mass flow rate through the fluid retention time in the heat dissipator wellbore and the heat losses in other sections of the y-shaped well couple. An optimum mass flow rate may be found to maximize the heat transfer into the NGH layer. This issue should be investigated in future studies.

The presented model does not consider the heat of phase transformation of the substance under reduced pressure conditions. In addition, the formation of gas phase due to NGH dissociation and gas production should reduce the thermal conductivity K of the reservoir, while the water phase dropped out from the dissociation may increase the thermal conductivity. The resultant effect should be investigated in laboratories and/or numerical simulation of the dynamic water-gas two-phase flow coupled with a heat–transfer mechanism. A fully coupled model for mass transfer and heat transfer should be developed in future studies.

6. Conclusions

An analytical model was developed in this study to describe the heat transfer process from wellbore to NGH reservoir for enhancing gas well productivity in NGH reservoirs. The following conclusions are drawn:

1. The analytical model was validated by a comparison of its result and the result given by a numerical model for an arbitrary data set. A comparison of temperature profiles given by the analytical and numerical models indicates that the results given by the two models are identical, which proves the correctness of the analytical model.
2. Applying the analytical model to the NGH reservoir in the Shenhu area, Northern South China Sea, allowed for predicting temperature profiles both in spatial and time domains. Model results reveal that the NGH reservoir temperature should increase quickly at any heat-affected point, but it should propagate slowly in the radial direction.
3. It should take more than two years to dissociate NGH within 20 m of the heat dissipator wellbore due to only thermal stimulation. Therefore, the geo-thermal stimulation method should be used as a technique for accelerating gas production with a depressurization scheme.
4. Because the real gas law demands that the increase in temperature will increase the pressure of free gas behind the NGH dissociation temperature (15 °C) front, it is expected that reformation of NGH may occur if the pressure fluctuates. This suggests that the natural gas released from the NGH should be produced in time through the gas production wellbore to reduce pressure.
5. The analytical model shows that, for a given system, the heat transfer is proportional to the mass flow rate and the temperature drop along the heat dissipator wellbore. Because this temperature drop is affected by the mass flow rate through fluid retention time in the heat dissipator wellbore and heat losses in other sections of the y-shaped well couple, an optimum mass flow rate may be found to maximize the heat transfer into the NGH layer. This needs further investigations in the future.

Author Contributions: Conceptualization, B.G.; methodology, B.G.; software, H.Z.; validation, B.G.; formal analysis, B.G.; investigation, B.G.; resources, B.G.; data curation, H.Z.; writing—original draft preparation, B.G.; writing—review and editing, H.Z.; visualization, H.Z.; supervision, B.G.; project administration, B.G.; funding acquisition, B.G. All authors have read and agreed to the published version of the manuscript.

Funding: This research was funded by BIRD Foundation grant number EC-19 Fossil Energy.

Institutional Review Board Statement: Not applicable.

Informed Consent Statement: Not applicable.

Data Availability Statement: Not applicable.

Acknowledgments: The authors are grateful to BIRD for funding the project "Safe, sustainable, and resilient development of offshore reservoirs and natural gas upgrading through innovative science and technology: Gulf of Mexico–Mediterranean", through Contract No. EC-19 Fossil Energy.

Conflicts of Interest: The authors declare no conflict of interest.

Appendix A Mathematical Modeling of Heat Transfer into Gas Hydrate Reservoirs

Assumptions. Consider the horizontal heat dissipator wellbore shown in Figure 1. The following assumptions are made for modeling the heat transfer process:

- The reservoir is homogeneous and isotropic with constant density, thermal conductivity, and specific heat.
- The reservoir is considered infinitely large as compared to the wellbore size.

Governing Equation. The governing equation of temperature is the commonly known diffusivity equation expressed as

$$\frac{1}{r}\frac{\partial}{\partial r}\left(r\frac{\partial T}{\partial r}\right) = \frac{1}{\beta}\frac{\partial T}{\partial t} \tag{A1}$$

where T is temperature in °C, r is distance from the wellbore center line in meter, t is time in second, and b is thermal diffusivity constant defined by

$$\beta = \frac{K}{\rho_s C_{ps}} \tag{A2}$$

where K is thermal conductivity in W/m-°C, r is density in kg/m^3, and C_{ps} is specific heat in J/kg-°C.

Boundary Conditions. The initial condition is expressed as

$$T = T_i \text{ at } t = 0 \text{ for all } r. \tag{A3}$$

where T_i is initial reservoir temperature. The boundary condition at the wellbore is expressed as

$$q_{r_w} = -K\left[\frac{dT}{dr}\right]_{r=r_w} \text{ for all } t, \tag{A4}$$

where q_{rw} is the rate of flow of heat per unit time per unit area of wellbore in J/s-m^2. For a circular wellbore with radius r_w and length L, the following relation holds true:

$$q_{r_w} = \frac{Q_{r_w}}{2\pi r_w L} \tag{A5}$$

where Q_{rw} is rate of flow of heat per unit time in J/s. Substituting Equation (A5) into Equation (A4) and rearranging the latter gives

$$\frac{Q_{r_w}}{2\pi LK} = -r_w\left[\frac{dT}{dr}\right]_{r=r_w} \text{ for all } t. \tag{A6}$$

Solution

The solution of Equation (A1) is sought by Boltzmann's transformation:

$$s = \frac{r^2}{4\beta t} \tag{A7}$$

so that

$$\frac{\partial s}{\partial r} = \frac{r}{2\beta t} \tag{A8}$$

and

$$\frac{\partial s}{\partial t} = -\frac{r^2}{4\beta t^2} \tag{A9}$$

Substituting Equations (A7) through (A9) into Equation (A1) and rearranging the latter give

$$\frac{dT}{ds} + s\frac{d}{ds}\left(\frac{dT}{ds}\right) = -s\frac{dT}{ds}. \tag{A10}$$

Let

$$\frac{dT}{ds} = T'. \tag{A11}$$

Then, Equation (A10) becomes

$$T' + s\frac{dT'}{ds} = -sT' \tag{A12}$$

or

$$\frac{dT'}{T'} = -\frac{s+1}{s}ds \tag{A13}$$

which is integrated to obtain

$$lnT' = -lns - s + c_1 \tag{A14}$$

where c_1 is an integration constant. This equation is rearranged to give

$$T' = c_2\frac{e^{-s}}{s} \tag{A15}$$

where c_2 is a constant.

Chain rule gives

$$r\frac{dT}{dr} = r\frac{dT}{ds}\frac{ds}{dr} \tag{A16}$$

Chain rule gives

$$r\frac{dT}{dr} = r\frac{dT}{ds}\frac{ds}{dr} = r\frac{dT}{ds}\left(\frac{r}{2\beta t}\right) = \frac{dT}{ds}\left(\frac{r^2}{2\beta t}\right) = 2s\frac{dT}{ds} \tag{A17}$$

Substituting Equation (A15) into Equation (A17) gives

$$r\frac{dT}{dr} = 2c_2e^{-s} \tag{A18}$$

At a wellbore where s approaches 0, this relation becomes

$$r_w\left[\frac{dT}{dr}\right]_{r=r_w} = 2c_2 \tag{A19}$$

Applying boundary condition Equation (A6) to Equation (A19) yields

$$\frac{Q_{r_w}}{2\pi LK} = -2c_2 \tag{A20}$$

which gives

$$c_2 = -\frac{Q_{r_w}}{4\pi LK} \tag{A21}$$

Substituting Equation (A21) into Equation (A15) gives

$$\frac{dT}{ds} = -\frac{Q_{r_w}}{4\pi LK}\frac{e^{-s}}{s} \tag{A22}$$

which is integrated over time:

$$\int_{T_i}^{T} dT = -\frac{Q_{r_w}}{4\pi LK}\int_{\infty}^{s}\frac{e^{-s}}{s}ds \tag{A23}$$

or

$$T = T_i - \frac{Q_{r_w}}{4\pi LK}\int_{\infty}^{s}\frac{e^{-s}}{s}ds = T_i + \frac{Q_{r_w}}{4\pi LK}\int_{s}^{\infty}\frac{e^{-s}}{s}ds \tag{A24}$$

i.e.,

$$T = T_i + \frac{Q_{r_w}}{4\pi LK}E_i(s) \tag{A25}$$

The heat flow rate from wellbore to reservoir can be calculated by

$$Q_{rw} = C_{pl}\dot{m}_p(T_{in} - T_{out}) \tag{A26}$$

where C_{pl} is the heat capacity of the fluid inside the wellbore in J/(kg·°C), $\dot{m}_p$ is the mass flow rate inside the wellbore in kg/s, and T_{in} and T_{out} are fluid temperatures in °C at the inlet and outlet of the wellbore, respectively.

References

1. U.S. Geological Survey Fact Sheet 021-01. Available online: https://pubs.usgs.gov/fs/fs021-01/fs021-01.pdf (accessed on 9 February 2022).
2. Demirbas, A. Methane hydrates as potential energy resource: Part 2–Methane production processes from gas hydrates. *Energy Convers. Manag.* **2010**, *51*, 1562–1571. [CrossRef]
3. Moridis, G.J.; Collett, T.S.; Boswell, R.; Kurihara, M.; Reagan, M.T.; Koh, C.; Sloan, E.D. Toward Production from Gas Hydrates: Current Status, Assessment of Resources, and Simulation-Based Evaluation of Technology and Potential. *SPE Reserv. Eval. Eng.* **2009**, *12*, 745–771. [CrossRef]
4. Sloan, E.D., Jr. *Clathrate Hydrates of Natural Gases*; Marcel Dekker, Inc.: New York, NY, USA, 1990; pp. 12–16.
5. Kurihara, M.; Funatsu, K.; Ouchi, H.; Masuda, Y.; Narita, H. Investigation on Applicability of Methane Hydrate Production Methods to Reservoirs with Diverse Characteristics. In Proceedings of the 5th International Conference on Gas Hydrates, Trondheim, Norway, 13–16 June 2005; Volume 3, pp. 714–725.
6. Macfarlane, A. *China Makes 'Flammable Ice' Breakthrough in South China Sea*; CNN Money: New York, NY, USA, 2017.
7. Zhang, W.; Bai, F.; Shao, M. Progress of offshore natural gas hydrate production tests in Japan and implications. *Mar. Geol. Quat. Geol.* **2017**, *37*, 27–33.
8. Konno, Y.; Fujii, T.; Sato, A. Influence of Flow Properties on Gas Productivity in Gas-Hydrate Reservoirs: What Can We Learn from Offshore Production Tests? *Energy Fuels* **2021**, *35*, 8733–8741. [CrossRef]
9. Paull, C.K.; Ussler, W.; Lorenson, T.; Winters, W.; Dougherty, J.; Iii, W.U. Geochemical constraints on the distribution of gas hydrates in the Gulf of Mexico. *Geo-Mar. Lett.* **2005**, *25*, 273–280. [CrossRef]
10. Wan, L.; Shaibu, R.; Hou, X.; Guo, B. A Feasibility Study of Producing Natural Gas from Subsea Hydrates with Horizontal Snake Wells. In Proceedings of the Paper OTC 29816-MS 2019 Offshore Technology Conference, Rio de Janeiro, Brazil, 29–31 October 2019; pp. e28–e31.
11. Guo, B.; Fu, C.; Liu, N. A priori assessment of long-term productivity of frac-packed wells for producing natural gas from marine gas hydrate reservoirs. *Energy Sci. Eng.* **2021**, *9*, 884–896. [CrossRef]
12. Mahmood, N.; Guo, B. Productivity comparison of radial lateral wells and horizontal snake wells applied to marine gas hydrate reservoir development. *Petroleum* **2021**, *7*, 407–413. [CrossRef]
13. Ekhator, E.; Guo, B. Assessing the effect of well completion types on productivity in a class 1G gas hydrate reservoir under pseudo steady state. *Petroleum* **2021**, *7*, 414–426. [CrossRef]

14. Max, M.D.; Johnson, A.H. *Exploration and Production of Oceanic Natural Gas Hydrate*; Springer International Publishing: Berlin/Heidelberg, Germany, 2016; pp. 39–73.
15. Ahmadi, G.; Ji, C.; Smith, D.H. Production of natural gas from methane hydrate by a constant downhole pressure well. *Energy Convers. Manag.* **2007**, *48*, 2053–2068. [CrossRef]
16. Li, X.; Xu, C.-G.; Zhang, Y.; Ruan, X.-K.; Li, G.; Wang, Y. Investigation into gas production from natural gas hydrate: A review. *Appl. Energy* **2016**, *172*, 286–322. [CrossRef]
17. Li, G.; Tang, L.G.; Huang, C.; Feng, Z.P.; Fan, S.S. Thermodynamic evaluation of hot brine stimulation for natural gas hydrate dissociation. *J. Chem. Ind. Eng. China* **2006**, *57*, 2033–2038.
18. Kawamura, T.; Ohtake, M.; Sakamoto, Y.; Yamamoto, Y.; Haneda, H.; Komai, T.; Higuchi, S. Experimental study on steam injection method using methane hydrate core samples. In Proceedings of the Seventh (2007) ISOPE Ocean Mining Symposium, Lisbon, Portugal, 1–6 July 2007; pp. 83–86.
19. Li, G.; Li, X.S.; Tang, L.G.; Li, Q.P. Control mechanisms for methane hydrate production by thermal stimulation. In Proceedings of the 6th International Conference on Gas Hydrates, Vancouver, BC, Canada, 6–10 July 2008.
20. Kawamura, T.; Yamamoto, Y.; Ohtake, M.; Sakamoto, Y.; Komai, T.; Haneda, H. Experimental study on dissociation of hydrate core sample accelerated by thermodynamic inhibitors for gas recovery from natural gas hydrate. In Proceedings of the 5th International Conference on Gas Hydrates, Trondheim, Norway, 13–16 June 2005.
21. Najibi, H.; Chapoy, A.; Haghighi, H.; Tohidi, B. Experimental determination and prediction of methane hydrate stability in alcohols and electrolyte solutions. *Fluid Phase Equilibria* **2009**, *275*, 127–131. [CrossRef]
22. Moridis, G.J.; Reagan, M.T. Strategies for gas production from oceanic class 3 hydrate accumulations, OTC-18865. In Proceedings of the Offshore Technology Conference, Houston, TX, USA, 30 April–3 May 2007.
23. Moridis, G.J.; Reagan, M.T. Gas production from oceanic class 2 hydrate accumulations, OTC 18866. In Proceedings of the Offshore Technology Conference, Houston, TX, USA, 30 April–3 May 2007.
24. Gaydukova, O.; Misyura, S.; Strizhak, P. Investigating regularities of gas hydrate ignition on a heated surface: Experiments and modelling. *Combust. Flame* **2021**, *228*, 78–88. [CrossRef]
25. Hong, H.; Pooladi-Darvish, M. Simulation of Depressurization for Gas Production from Gas Hydrate Reservoirs. *J. Can. Pet. Technol.* **2005**, *44*, 39–46. [CrossRef]
26. Qin, X.; Liang, Q.; Ye, J.; Yang, L.; Qiu, H.; Xie, W.; Liang, J.; Lu, C.; Lu, H.; Ma, B.; et al. The response of temperature and pressure of hydrate reservoirs in the first gas hydrate production test in South China Sea. *Appl. Energy* **2020**, *278*, 115649. [CrossRef]
27. Moridis, G.J.; Collett, T.S.; Dallimore, S.R.; Inoue, T.; Mroz, T. Analysis and Interpretation of the Thermal Test of Gas Hydrate Dissociation in the JAPEX/JNOC/GSC et al. Mallik 5L-38 Gas Hydrate Production Research Well. In *Scientific Results from the Mallik 2002 Gas Hydrate Production Research Well Program*; Dallimore, S.R., Collett, T., Eds.; Geological Survey of Canada, Bulletin 585: Mackenzie Delta, NT, Canada, 2005.
28. Guo, B.; Shaibu, R.; Yang, X. Analytical Model for Predicting Productivity of Radial-Lateral Wells. *Energies* **2020**, *13*, 6386. [CrossRef]
29. Fu, C.; Guo, B.; Shan, L.; Lee, J. Mathematical modeling of heat transfer in y-shaped well couples for developing gas hydrate reservoirs using geothermal energy. *J. Nat. Gas Sci. Eng.* **2021**, *96*, 104325. [CrossRef]
30. Su, M.; Yang, R.; Wu, N.Y. Structural characteristics in the Shenhu Area, northern continental slope of South China Sea and their influence on gas hydrate. *Acta Geol. Sin.* **2014**, *88*, 318–326.
31. Li, J.-F.; Ye, J.-L.; Qin, X.-W.; Qiu, H.-J.; Wu, N.-Y.; Lu, H.-L.; Xie, W.-W.; Lu, J.-A.; Peng, F.; Xu, Z.-Q.; et al. The first offshore natural gas hydrate production test in South China Sea. *China Geol.* **2018**, *1*, 5–16. [CrossRef]
32. Guo, B.; Ghalambor, A. *Natural Gas Engineering Handbook*, 2nd ed.; Gulf Publishing Company: Houston, TX, USA, 2012; pp. 277–279. [CrossRef]